

# UNDERSTANDING THE OPERATION AND USE OF HIGH TEMPERATURE ELECTROCHEMICAL CORROSION RATE PROBES

Bernard S. Covino, Jr., Sophie J. Bullard, Stephen D. Cramer, Gordon R. Holcomb,  
and Małgorzata Ziomek-Moroz  
U.S. Department of Energy  
Albany Research Center  
Albany, OR  
1450 Queen Ave, SW  
Albany, OR 97321

Michael S. Cayard and David A. Eden  
InterCorr International Inc.  
14503 Bammel North Houston, Suite 300  
Houston, TX 77014

## ABSTRACT

Electrochemical corrosion rate probes were constructed and tested along with mass loss coupons in a  $N_2/O_2/CO_2$  plus water vapor environment. Temperatures ranged from 450° to 600°C. Corrosion rates for ash-covered mild steel, 304L SS, and 316L SS probes using electrochemical techniques were a function of time, temperature, and process environment. Correlation between electrochemical and mass loss corrosion rates was good.

**Keywords:** corrosion, coal combustion, gaseous, electrochemical noise, harmonic distortion, linear polarization resistance, high temperature.

## INTRODUCTION

Increasing the efficiency of the Rankine cycle in coal combustors can be accomplished by increasing heat exchanger steam temperatures and pressures, as is done in supercritical and ultra supercritical units. The benefits of increasing energy conversion efficiencies are reduced consumption of fossil fuels (coal, oil, and gas) and reduced emission of greenhouse gases ( $CO_2$ ). In order to achieve both of these benefits, it is necessary to overcome technological challenges related to materials of construction. New materials or material/coating combinations with adequate strength, creep, fatigue, and corrosion resistance will need to be developed. Additional issues are present when alternate fuels are used. While heat exchanger tubes in a coal-fired plants using clean high quality fuel may last 20 to 30 years, tubes in coal-fired plants using lower quality fuel and in some coal gasification plants last only 3 to 5 years.

Problems occur when equipment designed for either oxidizing or reducing conditions is exposed to alternating oxidizing and reducing conditions. The use of low  $NO_x$  burners is becoming more commonplace and can produce reducing environments that accelerate corrosion. Complicating the development of corrosion-resistant materials for fireside applications is the influence of ash deposits and thermal gradients on the corrosion mechanism. Ash deposits and thermal gradients have a synergism that greatly increases the corrosive attack on heat exchanging equipment such as waterwalls, reheaters, and superheaters. One method of addressing corrosion of these heat exchange surfaces is the use of corrosion sensors to monitor when process changes cause corrosive conditions. In such a case, corrosion rate could become a process control variable that directs the operation of a coal combustion or coal gasification system. Alternatively, corrosion sensors could be used to provide an indication of total metal damage and

thus a tool to schedule planned maintenance outages.

A number of research efforts have been aimed at developing high temperature corrosion probes for various industries. The majority of the research has been based on the use of electrochemical noise (EN)<sup>1-6</sup> techniques. Others have considered the use of electrochemical impedance spectroscopy (EIS)<sup>3-5</sup> and linear polarization resistance (LPR)<sup>6</sup>, zero resistance ammetry (ZRA)<sup>4</sup>, and electrical resistance (ER)<sup>4</sup>. However, only a limited effort has been made to quantify<sup>2</sup> the operation of corrosion rate probes. For these probes to be accepted routinely in the power generation industries, it is necessary to determine if they accurately measure corrosion and the changes in corrosion rate that occur in environments of interest, if the sensor materials have an optimum composition for the intended exposure, and if the sensitivity or accuracy of the sensor changes with exposure time in fireside environments. Once this is established, electrochemical corrosion rate sensors can be used extensively and will allow corrosion rate to become a process variable for power plant operators.

Most electrochemical corrosion rate measurement techniques measure a resistance that is representative of the rate of the corrosion reaction. This is true of the LPR, EN, and EIS techniques. These resistances are related to corrosion rate by the Stern-Geary linear approximation to the Butler-Volmer equation,

$$i_{\text{corr}} = B/R_p = B/R_n \quad (1)$$

where  $R_p$  is obtained from the LPR and EIS techniques,  $R_n$  is obtained from the EN technique,  $B$  is the Stern-Geary constant, and  $i_{\text{corr}}$  is the corrosion current density from which a corrosion rate may be calculated. The Stern-Geary constant is the only variable that is normally not measured, but commonly assumed to be a value of 0.020 to 0.030 V/decade. Because  $B$  is related to Tafel constants, it can be measured using either standard electrochemical polarization techniques or the harmonic distortion analysis (HDA) technique that is used in this report.

The purpose of the research presented here is to address some of the issues that impact the understanding and the use of electrochemical corrosion rate probes. This report is part of an effort to characterize the long-term stability and performance of probes, and to optimize the choice of sensor materials.

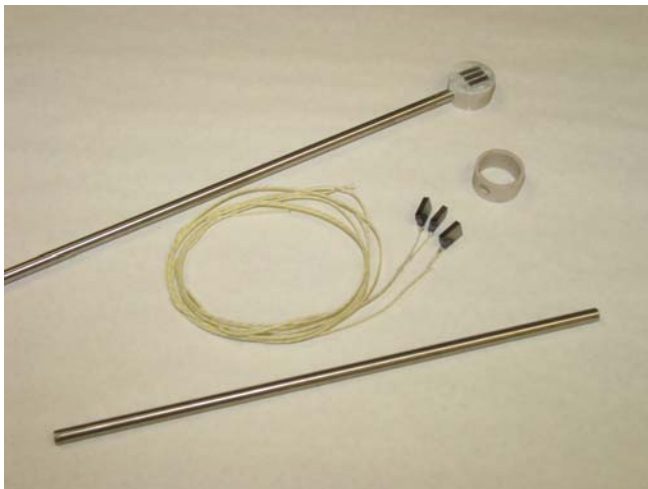


**Figure 1 – A completed high temperature corrosion rate probe and the components of construction.**

## EXPERIMENTAL DETAILS

Electrochemical corrosion rate (ECR) probes were designed and constructed for laboratory experiments using 4130 carbon steel (CS), 304L stainless steel (SS), and 316L SS sensors or electrodes. The probes were covered with ash and exposed, along with mass loss coupons made from the same material, to a mixed gas environment and temperatures that ranged from 450 to 600°C. The purpose was to determine the operating characteristics of probes and to compare integrated corrosion rates obtained probes to those obtained from mass loss coupons.

Three-sensor electrochemical corrosion rate probes were fabricated using the components shown in Figure 1. The cylindrical piece of ceramic served as the form to contain the sensors. The stainless steel tubing served to isolate the wires from the test environment and provided a path for the wires to exit the high temperature environment. Sensors were embedded within the ceramic form using a water-based

high-alumina cement. Final preparation included hand polishing the sensors to a 600 grit finish. The finished probe is shown in Figure 1.



**Figure 2 – Electrochemical corrosion rate probe and mass loss coupons prior to testing but after the application of a layer of ash. One coupon (far right) intentionally ash free.**

Experiments were conducted using an ash and a mixed gas environment identical to those reported previously<sup>7</sup>. The ash was obtained from a municipal incinerator and analyses showed high concentrations of corrosion-causing elements such as S, Cl, Pb, and K. The gas mixture consisted of 68 vol% N<sub>2</sub>, 15 vol% H<sub>2</sub>O, 9 vol% O<sub>2</sub>, and 8 vol% CO<sub>2</sub> with temperatures of 500 to 600°C. Typical test periods were 100 to 120 hours. An additional experiment designed to test the qualitative response of the CS ECR probes was conducted using coal gasifier ash, 78 vol% N<sub>2</sub>, 22 vol% O<sub>2</sub>, and temperatures of 200 to 700°C.

Tests designed to determine the quantitative nature of ECR probes involved exposing four mass loss coupons and the probe to the corrosive environment. Three of the four mass loss coupons were coated with ash on one side while one was left ash free. A slurry of the ash was applied to each of the ash-covered coupons and to the probe. Water was originally used to make the ash slurry; however, methanol was used for later tests. The ash-free coupon provided a corrosion rate used to correct the ash-covered coupon corrosion rates for corrosion of the ash-free side. Two of the ash-covered coupons were used to determine the mass loss corrosion rate for comparison to the ECR probe corrosion rate. The third ash-covered coupon was cross-sectioned for analyses to provide mechanistic information. Figure 2 shows the ash-covered probe and ash-covered and ash-free mass loss coupons.

Following exposure to the corrosive environment, ash was scraped from the surface in preparation for chemical cleaning. 4130 CS mass loss coupons were cleaned at 60°C in a 12 vol% H<sub>2</sub>SO<sub>4</sub> plus 0.25 vol% Rodine 95 (inhibitor) solution; the 304L and 316L SS mass loss coupons were cleaned at 25°C in a 10 vol% HNO<sub>3</sub> solution containing 2 vol% HF.

The corrosion measurement equipment used for this research was the SmartCET system<sup>(1)</sup>. This system applies three techniques, EN, LPR, and HDA, to the measurement of corrosion. The application of the three techniques and the appropriate data analysis produces a set of corrosion measurements approximately every 7 minutes. Data, which include EN, LPR, and HDA corrosion rates, an EN pitting factor, and Tafel and Stern-Geary constants from the HDA technique, are collected, displayed, and stored using FieldCET software<sup>(1)</sup>. A number of other variables, such as solution resistance, are collected and available for use. The ECR probe corrosion rates were determined by integrating the corrosion rates

<sup>(1)</sup> InterCorr International, Houston, TX, USA.

measured every 7 minutes to calculate the mass loss which was then divided by exposure time.

## RESULTS

### Qualitative Response of ECR Probes

Corrosion rates (mm/y) as a function of time, temperature, and water vapor content are shown in Figure 3 for an ash-covered 4130 CS ECR probe exposed to air. The relatively high corrosion rate at the beginning of the experiment is thought to be due to the abundance of water present in the slurry-added ash. Note that after the temperature exceeded approximately 200°C the corrosion rate decreased rapidly from 10 to approximately 0.02 mm/y. This is due to the drying of the ash. The corrosion rate in this experiment appears to respond well to increases and decreases in temperature. Water concentration up to 10% did not seem to affect the measured corrosion rate in a positive manner, but there was a significant decrease in corrosion rate when the water was unintentionally turned off at approximately 90 hours after the start of the experiment. The addition of 15% water after the temperature reached 700°C appeared to have a significant effect on the corrosion rate. It is well known that water vapor causes accelerated corrosion in some high temperature environments<sup>8</sup>.

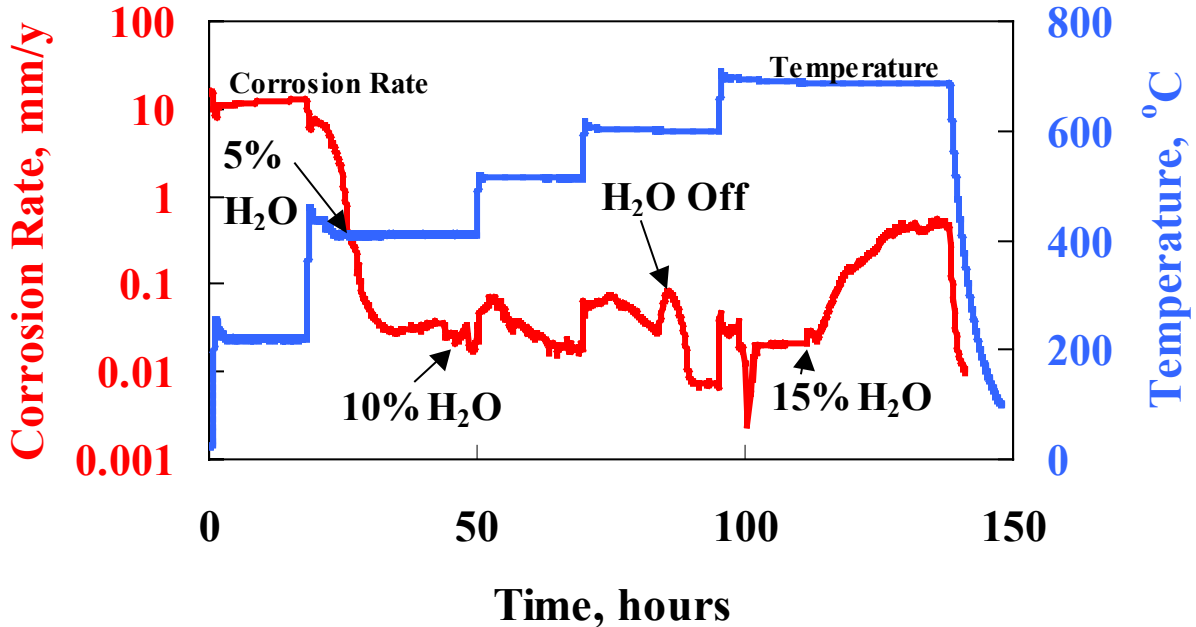


**Figure 3 - Effect of time and temperature and the addition of water vapor on the corrosion rate of mild steel.**

A pitting or localized corrosion factor and the Stern-Geary constant (B) were measured for the experiment shown in Figure 3. Pitting factor showed no correlation to any of the process variable changes and was low, below 0.01, for the majority of the experiment. Interpretation of pitting and the pitting factor at high temperatures is not routine and will require more research to determine what the pitting factor represents in such cases. The average Stern-Geary factor measured for this experiment was 0.0117 V/decade, a value much lower than the 0.020 to 0.030 V/decade that is commonly assumed for corrosion processes. One use for this measured value of B is to allow a more accurate calculation of corrosion rate when using equation (1). The Stern-Geary constant and the Tafel constants that are used to

calculate B can also be coupled with other information, such as scale analyses and electrochemical data from other techniques, to help explain corrosion mechanisms.

#### Quantitative Nature of ECR Probes

The data in Figure 3 represents qualitative changes the corrosion process. At present, there is no way of knowing whether the numbers measured are actual corrosion rates or the rates of other reactions. For that reason, experiments were conducted to compare electrochemical corrosion rates with actual mass loss corrosion rates for coupons and probes exposed in exactly the same environment. Six of these experiments are reported here. The first two used mild steel mass loss coupons and probes coated with ash and exposed to the  $N_2/O_2/CO_2/H_2O$  environment at 450 and 500°C. Graphs showing temperature and corrosion rate as a function of time are given in Figures 4 and 5 for a 450°C test. For all of this data the corrosion rates were calculated using the LPR data and the Stern-Geary constant (B) measured by the HDA technique. An average value of  $B = 0.012$  V/decade was measured for both the 450°C and the 500°C tests.

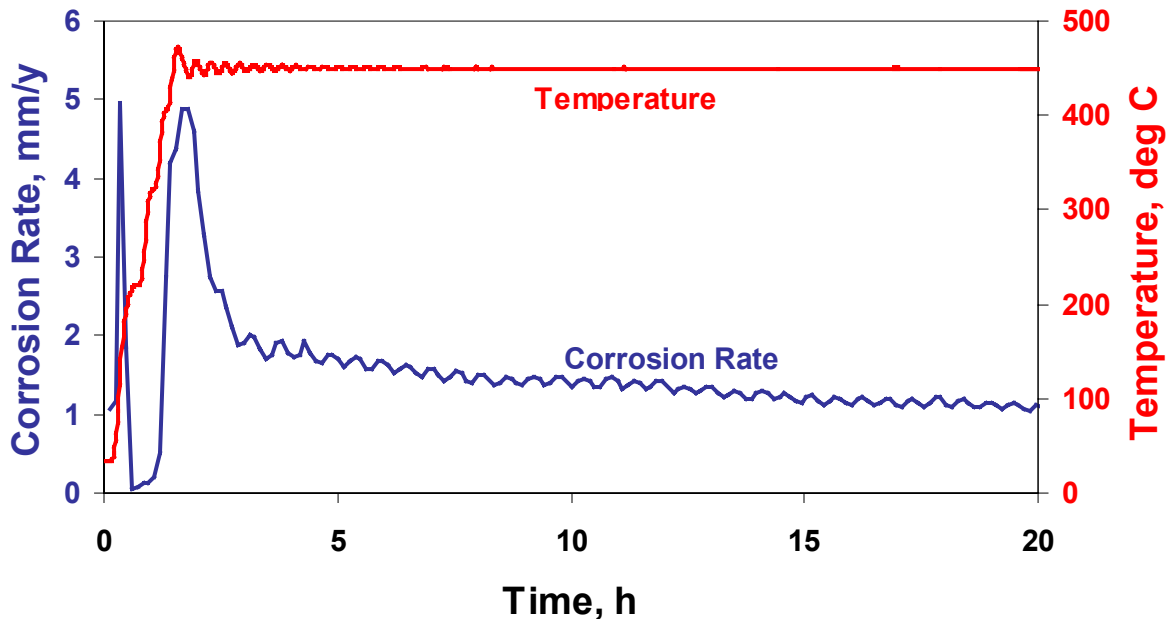


**Figure 4 – Expanded view of the exposure of 4130 CS to the  $N_2/O_2/CO_2/H_2O$  environment at 450°C.**

The response of the mild steel ECR probe was similar at both temperatures. Figure 4 shows an expanded view of the first 20 hours the 450°C experiment. There was some instability, very high and very low corrosion rates, during the heat up process. As discussed above, some of this may be due to the drying out of the ash as temperature increased. Both sets of data also showed periodic oscillations in the measured corrosion rate, which were coincidental with oscillations in the furnace temperature. Temperature fluctuated  $\pm 0.5^\circ\text{C}$  over 30 minute cycles, causing the measured corrosion rate to cycle also. Long-term corrosion rates in Figures 5 decreased with time as expected for metals that form protective or semi-protective scales.

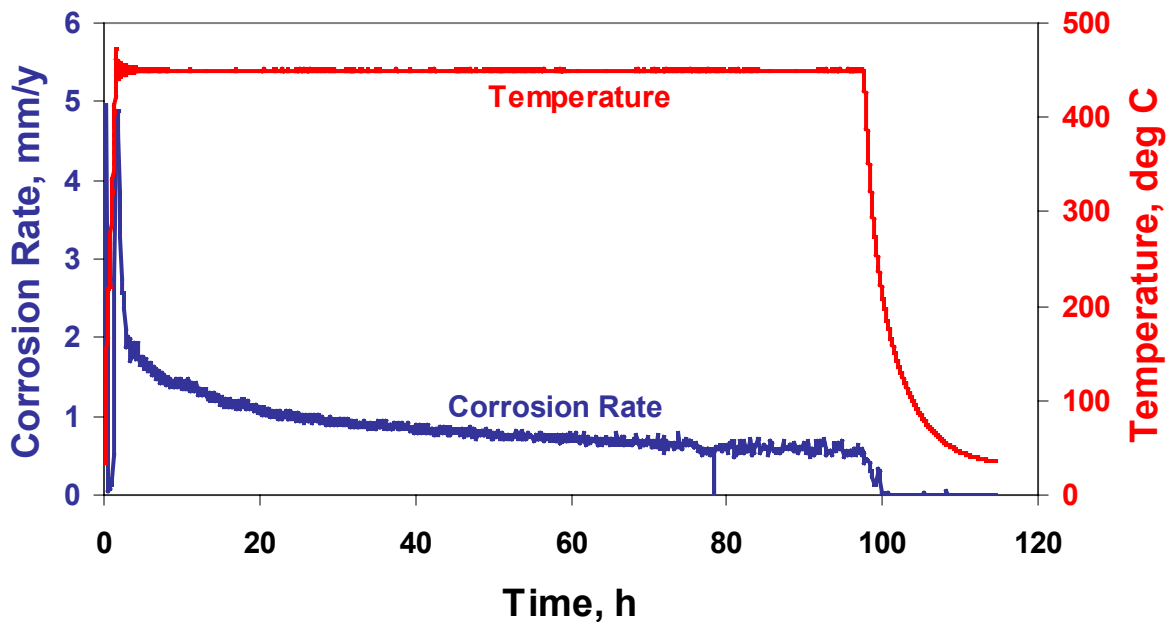


Figure 5 - Complete data for the 450°C exposure of 4130 CS.

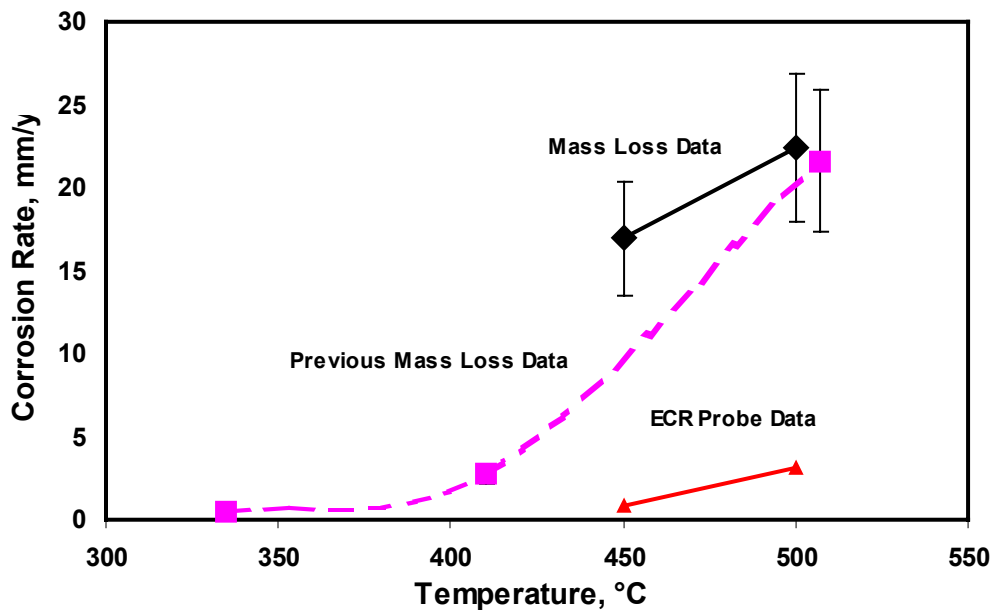


Figure 6 - Comparison of ECR probe and mass loss corrosion rates.

Mass loss coupons were cleaned of all ash and scale and corrosion rates were calculated. This data is shown in Figure 6 and compared to 120-hour corrosion rates reported previously<sup>7</sup> for a mild steel (UNS K01200) boiler tube in the same environment. The results showed that the mass loss corrosion rates for the research reported here were similar, but not identical, to those reported previously<sup>7</sup>. There was a 20% variability in the measured mass loss corrosion rates (note the error bars in Figure 6), which

accounts for some of the differences in the two studies. However, the results from both studies are close enough to state that the actual mass loss corrosion rates are close to the values shown in Figure 6.

The data in Figure 5 was integrated to determine a cumulative mass loss. This was then used to calculate a corrosion rate for the ECR probe. The electrochemical corrosion rates shown in Figure 6 do not compare well with the mass loss corrosion rates. They show a similar trend and slope but the ECR probe corrosion rates are significantly lower than the mass loss corrosion rates.

The second and third types of coupons tested, 304L and 316L SS mass loss coupons and electrochemical corrosion rate probe, were coated with ash and exposed to the same N<sub>2</sub>/O<sub>2</sub>/CO<sub>2</sub>/H<sub>2</sub>O environment but at 500 and 600°C. The ECR probe response to temperature and exposure time was qualitatively similar to that shown in Figures 4 and 5. Corrosion rates increased during the heat-up period and then decreased with time to the end of the exposure period. At the end of the experiments when the gases and H<sub>2</sub>O were turned off and the temperature reduced to 20°C, corrosion rates decreased rapidly.

**Table 1 – Stern-Geary constants measured by the HDA technique.**

Alloy	Stern Geary Constant (B), V/decade		
	450°C	500°C	600°C
4130 CS	0.0117	0.0130	–
304L SS	–	0.0156	0.0182
316L SS	–	0.0130	0.0130

– = not measured

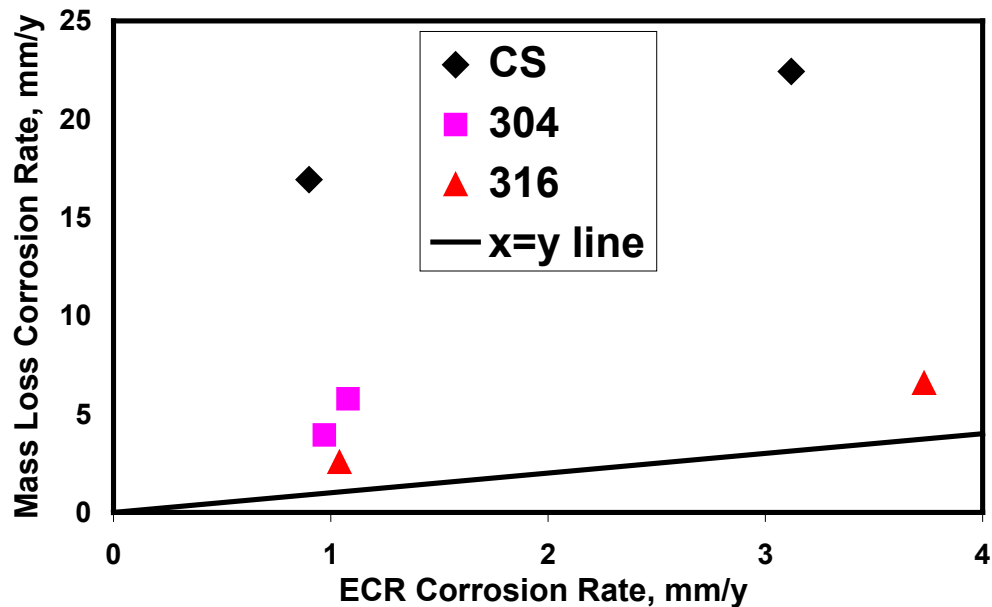


**Figure 7 - Comparison of mass loss to ECR probe corrosion rates.**

The Stern-Geary constants measured for all of the experiments are reported in Table 1. These ranged from 0.0117 to 0.0182 V/decade with an average value of 0.0141V/decade. This average is significantly lower than the normally assumed values of 0.020 to 0.030 V/decade. The actual values in Table 1 were used to calculate the ECR probe corrosion rates that are shown in Figure 7 plotted against the mass loss corrosion rates.

There are several interesting observations that can be made from Figure 7. Mass loss corrosion rates are all greater than the ECR probe corrosion rates. These differences vary from a factor of 2 to a factor of 19. The greatest differences are for 4130 CS, followed by 304L SS and 316L SS. The agreement appears to be better for the more highly alloyed material, 316L SS. In fact, the mass loss corrosion rates ranged from 2 to 2.5 times higher than the ECR probe corrosion rates for 316L SS.

## DISCUSSION

Results presented here show that mass loss corrosion rates are generally a factor of 2 or more greater than ECR probe corrosion rates. Studies<sup>9</sup> conducted using different conditions (probe construction, coating, and gaseous environment) but with the same SmartCET equipment had better agreement between ECR probe and mass loss corrosion rates. This suggests that there may be other factors that need to be understood when using ECR probes. Some possible factors are discussed below:

Stern Geary constant – The choice of the Stern-Geary (B) constant may be the most powerful factor affecting reported electrochemical corrosion rates. As can be seen in equation 1, corrosion rate is directly proportional to B. Within reason, a B value could be chosen to make the ECR probe corrosion rates coincide with mass loss corrosion rates. This was not done in this report, rather the B values measured using the HDA technique, Table 1, were used. This may be one reason why corrosion rates measured by the two techniques differed. Other studies<sup>1,2</sup> of ECR probes did not report the method used to calculate corrosion rates or the value of B used.

Mass loss corrosion rates – In attempting to correlate ECR probe corrosion rates with mass loss corrosion rates, it is important that the mass loss measurements be as accurate as possible. This requires enough coupons to ensure a statistically significant average corrosion rate. Another factor is the difficulty of determining corrosion rates using mass loss coupons that are coated with ash on only one side, as were used in this report. There will always be uncertainties when trying to partition a corrosion rate between the ash-coated and the ash-free side. Future experiments should be conducted on coupons totally encapsulated in ash.

Other researchers<sup>2</sup> have used EN probe data and profilometry to measure the corrosion penetration rate of their probe surfaces in an effort to quantify their electrochemical corrosion rates. Still others<sup>4</sup> have used EIS data for the probe measurement and the SEM to measure the metal lost from the actual probe. Both of these research groups generated mass loss and electrochemical probe corrosion rates that differed by only about 50%. This is in comparison to the differences for our data presented in Figure 7.

Probe construction – Two factors related to the design of the probe are: a good seal between the potting compound and the sensor electrodes and a high-resistivity potting compound at elevated temperatures. The former prevents corrosion from penetrating down the sides of the sensors thus increasing the exposed metal area. This will cause a higher ECR probe corrosion current and thus a higher corrosion current density or corrosion rate. The later will prevent leakage current or cross talk between the sensors. This also would cause a higher ECR probe corrosion rate.



Internal corrosion – Electrochemical corrosion rates are based on measuring the current generated during the conversion of metals to metal ions for general corrosion processes. When internal corrosion processes occur, however, the corrosion penetrates into the metal leaving unconsumed metal grains. Figure 8 shows a cross-sectional view of a 304L SS coupon exposed as part of the research reported here. Note the penetration of the internal corrosion around the grains near the top surface.

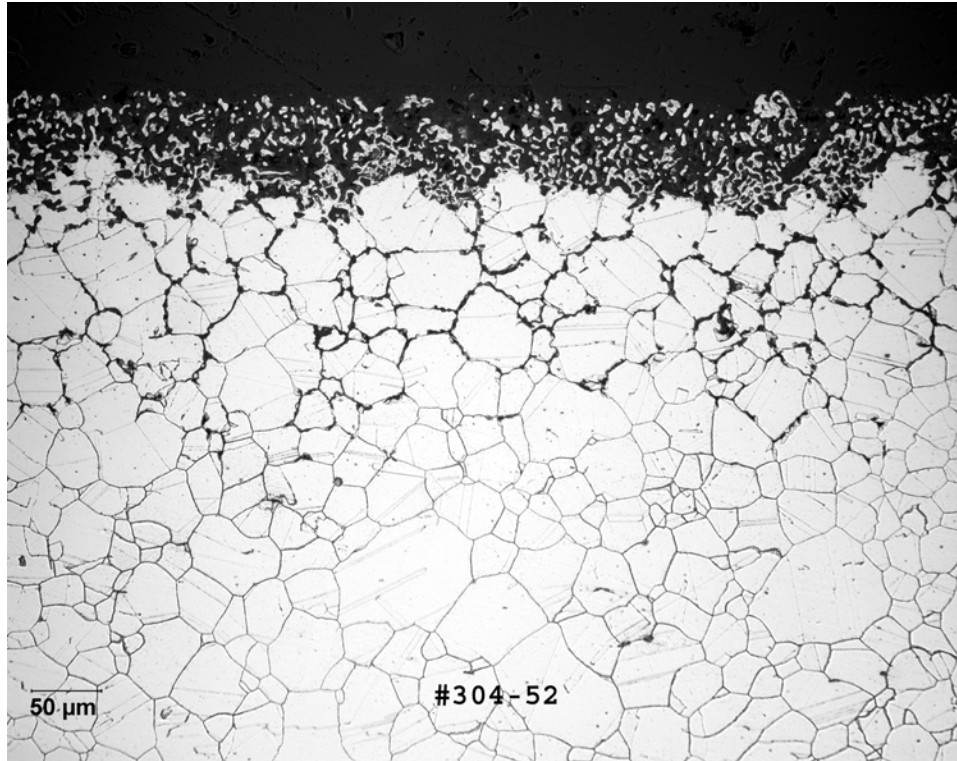


**Figure 8 - Cross-section of 304 SS showing internal corrosion.**

This would affect the mass loss corrosion rates in the following way. During de-scaling or pickling of the corroded coupons, the un-reacted metal grains shown in Figure 8 could be removed as the internal corrosion is dissolved by the pickling solution. This would cause the mass loss corrosion rates to be higher than that measured electrochemically.

Ash or scale properties - It has been suggested that electrochemical corrosion rate measurements could not be made in the presence of an electrically conductive scale. In that situation only the resistance of the scale will be measured<sup>5</sup>. It is possible that the corrosion scale or the ash used to coat the probes reported here were electrically conductive and that this affected the measured corrosion rates.

## CONCLUSIONS

- LPR-based electrochemical corrosion rate probes are able to measure corrosion rates that are sensitive to temperature and process changes.
- The HDA technique is able to measure a unique value of the Stern-Geary constant in high temperature corrosion environments.
- There were relatively large differences between the mass loss and electrochemical probe corrosion rates for the 4130 CS coupons and probes.

- Both 304L and 316L SS produced ECR probe corrosion rates that were similar to their mass loss corrosion rates.
- Selection of the Stern-Geary constant, internal corrosion, mass loss corrosion techniques, probe construction, and ash chemistry are possible factors that can influence mass loss and ECR probe corrosion rates.

## REFERENCES

1. T.M. Linjeville, K.A. Davis, G.C. Green, W.M. Cox, R.N. Carr, N.S. Harding, and D. Overacker, "On-Line Technique for Corrosion Characterization in Utility Boilers, Proceedings of Power Production in the 21st Century: Impacts of Fuel Quality and Operations," United Engineering Foundation, Snowbird, UT, October 28-November 2, 2001.
2. T.M. Linjeville, J. Valentine, K.A. Davis, N.S. Harding, and W.M. Cox, "Prediction and Real-time Monitoring techniques for Corrosion Characterization in Furnaces," *Materials at High Temperatures*, Vol. 20, No. 2, pp. 175-184, 2003.
3. D.M. Farrell, W.Y. Mok, and L.W. Pinder, "On-line Monitoring of Furnace-Wall Corrosion in a 125 MW Power Generation Boiler," *Materials Science and Engineering*, Vol. A121, pp. 651-659, 1989.
4. D. M. Farrell, "On-line Monitoring of Fireside Corrosion in Power Plant," 12<sup>th</sup> International Corrosion Congress, Vol. 12, pp. 4131-4140, 1993.
5. G. Gao, F.H. Stott, J.L. Dawson, and D.M. Farrell, "Electrochemical Monitoring of High-Temperature Molten Salt Corrosion," *Oxidation of Metals*, Vol. 33, Nos. 1/2, pp. 79-94, 1990.
6. G.J. Bignold and G.P. Quirk, "Electrochemical Noise Measurements in a 500 MW Steam Turbine to Maximize Lifetime Under Changing Operational Demands," Paper no, 02333, CORROSION/2002, NACE International, Houston, TX, 20 pp, 2002.
7. B. S. Covino, Jr., J. H. Russell, S. D. Cramer, G. R. Holcomb, S. J. Bullard, M. Ziomek-Moroz, S. A. Matthes, and M. L. White, "The Role of Ash Deposits in the High Temperature Corrosion of Boiler Tubes," Paper no.03718, CORROSION/2003, NACE International, Houston TX, 12 pp., 2003.
8. F. H. Stott and J. F. Norton, "Laboratory Studies involving Corrosion in Complex, multi-component Gaseous Environments at Elevated Temperatures," in *Corrosion in Advanced Power Plants*, Proceedings of the Second International Workshop on Corrosion in Advanced Power Plants, pp. 43-51, 1997.
9. D. A. Eden and B. Breene, "On-Line Electrochemical Corrosion Monitoring in Fireside Applications," Paper No. 03361, CORROSION/2003, NACE International, Houston, TX, 10 pp., 2003.